Induction of G_1 arrest in glioma cells by T11TS is associated with upregulation of Cip1/Kip1 and concurrent downregulation of cyclin D (1 and 3)

Sagar Acharya, Sirshendu Chatterjee, Pankaj Kumar, Malabika Bhattacharjee, Suhnrita Chaudhuri and Swapna Chaudhuri

In our laboratory, a novel therapeutic probe, T11TS, a membrane glycoprotein, was isolated which had antineoplastic activity against experimental glioma. Development of a novel therapeutic strategy with T11TS has unearthed a newer dimension of its mechanism of action: modulation of the cell cycle. In this study, we have presented evidence to support the finding that T11TS induces G_1 cell cycle arrest of rat glioma cells. Results of flow cytometric studies showed that the treatment produced a marked increase in the proportion of cells in the G_1 phase. Flow cytometry, immunoblotting, immunoprecipitation, and kinase assays were performed for investigating the involvement of G_1 cell cycle regulators. T11TS induces downregulation of the cyclin-D (1 and 3) expression with the concurrent upregulation of $p21^{Cip1}$ and $p27^{Kip1}$ and their concomitant association with cyclin-dependent kinase 4, proliferating cell nuclear antigen and cyclin E respectively leading to a decrease in cyclin-dependent kinase 4 kinase activity. A transient rise in retinoblastoma protein level and coordinated binding of retinoblastoma protein with E2F coincided with the accumulation of cells in G_1 phase. Thus, our observations have uncovered an antiproliferative pathway for T11TS, causing retardation of glioma cell cycle. *Anti-Cancer Drugs* 21:53–64 © 2010 Wolters Kluwer Health | Lippincott Williams & Wilkins.

Anti-Cancer Drugs 2010, **21**:53–64

Keywords: cyclin, cyclin-dependent kinase, glioma, $p21^{Cip1}$, $p27^{Kip1}$, T11TS

Department of Laboratory Medicine, School of Tropical Medicine, Kolkata, West Bengal, India

Correspondence to Professor Swapna Chaudhuri, PhD, Head, Department of Laboratory Medicine, School of Tropical Medicine, 108, C.R. Avenue, Kolkata 700073, India
Tel: +91 033 2241 4065 x207, +91 033 2257 2938 (O);
fax: +91 033 2241 4915; e-mail: swapna.chaudhuri@gmail.com

Received 20 July 2009 **Revised form accepted** 31 August 2009

Introduction

Malignant gliomas, the most common subtype of primary brain tumors, are aggressive, highly invasive and are considered the deadliest of human cancers. The fundamental biological features of malignant gliomas in humans, including their diffusely infiltrative nature and their remarkable propensity toward further malignant progression, have been among the major impediments to developing successful therapies [1].

Overproliferation of certain cells is the basis for tumor formation and therefore impairment of the regulation of the cell cycle are inalienable and basic signs of tumor cells. Activities of sequential cyclin-dependent kinases (CDKs) are the 'motor' of the cell cycle [2]. Regulation of CDK activity occurs through directed changes in certain cyclins during cell cycle phases [3]. Cyclin D isoforms associate with CDK4 and CDK6 and this association leads to the activation of CDK4 and CDK6, which help in maintaining and progressing through the early G_1 phase of the cell cycle [4,5]. Cyclin E and CDK2 proteins play a role in the transition from the G_1 to S phase of the cell cycle [6]. The G_1-phase-specific cyclin and CDK complexes phosphorylate the retinoblastoma protein (pRb) and repress its inhibitory activity by associating with the E2F transcription factor, which mediates the expression of S-phase-specific genes [7]. The mammalian Rb family includes Rb, Rb1/p107 and Rb2/p130 proteins, which are highly related in amino acid sequence and function [8,9]. The primary kinase responsible for Rb phosphorylation is D-type cyclin-dependent kinase [4]. Cyclin E/CDK2 also functions to further the process of Rb inactivation that was initiated by cyclin D/CDK4 action. Thus, virtually the entire process involved in the activation of DNA replication and the regulation of the G_1/S transition is under the control of the Rb/E2F pathway [10,11]. Cyclin D/CDK4 activity is induced by growth stimulation, thus initiating the cascade of events that leads to E2F accumulation and S-phase entry [7].

The activity of CDK/cyclin complexes can be negatively regulated by cyclin-dependent kinase inhibitors (CDKIs). p21Waf1/Cip1 ($p21^{Cip1}$) and $p27^{Kip1}$ belong to the family of CDK inhibitors (CDKIs) [12,13] whose expression regulates the G_1-phase CDKs [14]. The members of the CIP/KIP family of CDK-regulatory molecules ($p21^{Cip1}$, $p27^{Kip1}$) comprise a class of polypeptides

All supplementary data are available directly from the authors.

0959-4973 © 2010 Wolters Kluwer Health | Lippincott Williams & Wilkins DOI: 10.1097/CAD.0b013e32833276e8

acting as broad-spectrum inhibitors of different cyclin–CDK complexes [12,13]. The passage through the G_1–S transition is absolutely dependent on cyclin E and its accumulation is one of the rate-limiting steps for entry into S phase. Several observations suggest that $p27^{Kip1}$ is sufficient to inhibit G_1 progression by targeting the cyclin E/CDK2 complex [6,7,13].

$p21^{Cip1}$, the pivotal member of the Waf1/CIP1 family of CDKIs, is induced in a p53-dependent manner in response to DNA damage [13], and is a critical determinant of the cell cycle arrest in G_1 [14,15]. Nevertheless, $p21^{Cip1}$ also responds to additional signals independent of p53 and has been implicated in terminal differentiation and senescence [16–18]. A conserved bipartite motif in the amino-terminal end of CKIs is required for binding and inhibition of cyclin–CDK complexes [19,20]. A unique feature of $p21^{Cip1}$ that distinguishes it from the other CKIs is its ability to associate with the proliferating cell nuclear antigen (PCNA), by an additional binding motif located near the carboxyl terminus [19,21,22]. PCNA is a cyclin and the DNA polymerase δ and ε auxiliary factor is synthesized at greater rate in the S phase of growing cells [23] and facilitates loading of the polymerases onto the DNA templates and increases their activity in both DNA replication and repair. Through an interaction with PCNA, $p21^{Cip1}$ inhibits PCNA-dependent DNA replication [24,25].

T11TS, a membrane glycoprotein, has been isolated from sheep red blood cell membrane [26]. Our group established, for the first time, that T11TS- mediated glioma abrogation in a rat model by T11TS-mediated immune potentiation in the immunosuppressive glioma state [27,28]. The multimeric recombinant form of T11TS has been shown to inhibit human T-cell proliferation [29], although the detailed cellular regulation by T11TS which brings about cell cycle arrest of glioma cells has not been determined.

In this study, we have shown that T11TS-mediated cell cycle arrest occurred at G_1 phase. Arrest is brought about by downregulation of cyclin D (1 and 3) and simultaneous upregulation of $p21^{Cip1}$ and $p27^{Kip1}$ through direct binding inhibits CDK4 and PCNA-dependent DNA replication in glioma cells.

Materials and methods

Animals

Healthy newborn Druckray rats, 2–3 days old of both sexes along with the mother, were maintained in our laboratory for the purpose of investigation. There were six animals in each group. They were weaned at 30 days of age and housed separately in isolated cages. All animals were fed autoclaved Vet care pellets and water and housed in a room with ambient temperature of 22°C in a 12 h light/darkness cycle. The animals were grouped into five groups, as follows:

(1) N: normal control,
(2) ENU: 3 to 5-day-old neonatal animals injected with ethyl nitrosourea (ENU) intraperitoneally (i.p.),
(3) ET1: 6-month-old ENU-treated animals injected (i.p.) with the first dose of T11TS,
(4) ET2: 6-month-old ENU-treated animals injected (i.p.) with the first and second doses of T11TS,
(5) ET3: 6-month-old ENU-treated animals injected (i.p.) with the first, second, and third doses of T11TS at an interval of 6 days for each dose.

Rats were examined daily and weighed weekly throughout the experimental period. Maintenance and animal experiment procedures strictly followed 'the Principles of Laboratory Animal Care' (NIH publication no. 85–23, revised in 1985) and also the local 'Ethics Regulations.'

Induction of brain tumor with ENU

N-N-ENU was freshly prepared by dissolving 10 mg/ml in sterile saline and adjusting the pH to 4.5 with crystalline ascorbic acid. ENU was injected i.p. to newborn rats (3–5 days old) with a dose of 80 mg/kg body weight [30,31].

Isolation of T11TS and administration in animals

T11TS was isolated from sheep erythrocyte (sheep red blood cell) membranes. Briefly, sheep red blood cells were trypsinized, treated with TCA and neutralized. The glycopeptides were separated by ion exchange chromatography on a DEAE-cellulose column and eluted with a five-gradient system. Elute fraction III was selected as the fraction of choice. The first dose of 1 ml of T11TS (0.4 mg/kg body weight) was administered to rats i.p. from the third elute fraction III, which was followed by a second booster dose on the sixth day and a third booster dose on the 12th day, making a dose schedule of 1, 2, and 3 ml to the ET1, ET2, and ET3 animals, respectively [28,32].

Isolation and purification of tumor cells

Oligodendroglioma and astrocytoma cells were isolated using the percoll gradient centrifugation technique. The method for isolating oligodendroglioma and astrocytoma cells was a modification of a percoll gradient centrifugation procedure. This cell isolation method separates oligodendroglioma and astrocytoma cells from a heterogeneous cell population by virtue of their cell density. Purity of isolated cells was checked by an anti-O4 antibody for oligodendrocytes and anti-glial fibrillary acidic protein antibody for astrocytes [33,34].

Flow cytometry analysis for cell cycle distribution

Harvested glioma cells (as described before) ($\sim 1 \times 10^5$ cells were taken to start with) were washed with cold phosphate-buffered saline (PBS), and processed for cell cycle analysis. Cells were fixed with 70% ethanol and the

samples were kept at 4°C overnight. After centrifugation, the pellet was washed twice with cold PBS, suspended in 500 µl PBS, and incubated with 5 µl RNase (20 µg/ml final concentration) for 1 h to ensure DNA staining. The cells were kept on ice for 15 min and incubated with propidium iodide (Sigma, Saint Louis, Missouri, USA) (50 µg/ml final concentration) for 1 h in the dark. The cell cycle distribution of each sample was then determined by using a FACS-Calibur instrument (BD Biosciences, San Jose, California, USA) equipped with CellQuestPro software (Becton Dickinson, San Jose, California, USA), which was used to determine the percentage of cells in the different phases of the cell cycle.

Expression of cell-cycle regulatory proteins by flow cytometry

Cell populations of approximately 1×10^6 cells/ml were treated with paraformaldehyde (0.3% in PBS) at 4°C for 1 h. Then the cell suspension was washed with cold PBS and collected to permeabilize the sample with Triton X-100 (0.5%) for 1 h at 4°C. After centrifugation, the pellet was washed twice with cold PBS and resuspended in 200 µl PBS. Cells were incubated with 1 µl of respective primary monoclonal antibody (Santa Cruz, California, USA) for 1 h at 4°C in the dark at a concentration of 1 µg monoclonal antibody per 1×10^6 cells (as per the recommendation of the manufacturer). Anti-cyclin D1, anti-cyclin D2, anti-cyclin D3, anti-cyclin E, anti-CDK2, anti-CDK4, anti-CDK6, anti-p16, anti-p21, anti-p27, anti-PCNA, and anti-Rb primary monoclonal antibody (Santa Cruz) were used to study the expression of respective protein levels in different groups. The anti-Rb antibody used was specific to the detection of total pRb. Cells were centrifuged, washed and resuspended in PBS and then incubated with secondary phycoerythrin-conjugated mouse IgG1 for 30 min in the dark. The isotype control was phycoerythrin-conjugated mouse IgG1; after incubation the cells were resuspended in PBS and subjected to flow cytometric analysis in FACS-Caliber instrument (BD Biosciences). A total of 10 000 events were acquired and analyzed.

Immunoblotting of cyclin D, cyclin E, CDK2, CDK4, CDK6, p16, $p21^{Cip1}$, $p27^{Kip1}$, p107, p130, E2F

Isolated cells were washed once with ice-cold PBS and lysed by incubating for 30 min on ice (2×10^7 cells/ml of lysis buffer) in NP-40 Cell Lysis buffer (20 mmol/l Tris–HCl pH 8.0, 137 mmol/l NaCl, 10% glycerol, 1% NP-40, 2 mmol/l EDTA, 50 µg/ml phenylmethylsulfonyl fluoride, 25 µg/ml aprotinin, 25 µg/ml leupeptin, 10 µg/ml trypsin inhibitor; Sigma). After centrifugation at 15 000 rpm for 15 min, the amount of protein was quantified by colorimetric assay. Of the total extracted proteins estimated by Bradford assay ($\lambda = 595$ nm), 50 µg were resolved in a 12% SDS–polyacrylamide gel and electrophoretically transferred to a PVDF membrane (Immobilon-PS^Q, Millipore, Billerica, Massachusetts, USA). The membrane was blocked with 5% nonfat milk–Tris-buffered saline Tween-20 TBST) (10 mmol/l Tris–HCl, 0.15 mol/l NaCl, 8 mmol/l sodium azide, 0.05% Tween-20, pH 8.0) containing 5% skim milk for 1 h at room temperature, and each primary antibody (diluted 1 : 1000 in blocking buffer) was applied overnight at 4°C in the same blocking solution. Anti-cyclin D1, anti-cyclin D2, anti-cyclin D3, anti-cyclin E, anti-CDK2, anti-CDK4, anti-CDK6, anti-p16, anti-p21, anti-p27, anti-PCNA, anti-p107, anti-p130, and anti-E2F monoclonal antibodies were used for the respective experiments (Santa Cruz). The anti-p107 and anti-p130 monoclonal antibodies used were specific for the detection of the hypophosphorylated form of Rb1 and Rb2 proteins. After incubation, membranes were washed fourr times with TBST and incubated with anti-mouse IgG-AP (diluted 1 : 10 000 in blocking buffer) for 1 h in blocking buffer at room temperature and washed four times for 5 min (per wash with TBST at room temperature). The membrane was then immersed in the 5-bromo-4-chloro-3-indolyl phosphate–nitro blue tetrazolium substrate solution. After approximately 15–20 min when the band began to appear (careful vigilance was maintained as the reaction time varied) the membrane was rinsed with distilled water to stop further development. The membrane was then scanned by Totallab (Phoretix, version 1.10). For every loading, β-actin was used as the loading control. Band detection and pixel intensity count were done by using Totallab (Phoretix, version 1.10; Nonlinear Dynamics, Newcastle, UK) software. Pixel intensity of the protein bands was deduced after deducting with respective loading control pixel intensity.

Immunoprecipitation

For immunoprecipitation experiments cells (10^7 cells) were washed twice with ice-cold PBS and harvested in 2 ml NP-40 lysis buffer (20 mmol/l Tris–HCl pH 8.0 137 mmol/l NaCl, 10% glycerol, 1% NP-40, 2 mmol/l EDTA, 50 µg/ml phenylmethylsulfonyl fluoride, 25 µg/ml aprotinin, 25 µg/ml leupeptin, 10 µg/ml trypsin inhibitor). Lysates were incubated for 30 min at 4°C. After centrifugation at 15 000 rpm for 15 min 1 mg of cellular extract, as determined by the Bradford assay ($\lambda = 595$ nm), was pre-cleared by incubating extracts with protein G agarose (Santa Cruz) for 1 h at 4°C. Pre-cleared extracts were then incubated with primary antibody (anti-p21 monoclonal antibody) overnight at 4°C and the immune complex was collected by incubation with protein G agarose (1 h at 4°C with rocking). Immunoprecipitates were washed four times with ice-cold PBS, eluted in 2 × SDS sample buffer and resolved in 12% SDS–polyacrylamide gel and for subsequent immunoblotting the same protocol was followed as described above. Anti-CDK4 monoclonal antibody (Santa Cruz) and anti-PCNA (Santa Cruz) monoclonal antibodies were used as a primary antibody (diluted 1 : 1000 in blocking buffer) to find whether any functional complex formed with $p21^{Cip1}$

– CDK4 and $p21^{Cip1}$ – PCNA. An anti-p27 monoclonal antibody was used to immunoprecipitate and anti-cyclin E monoclonal antibody (Santa Cruz) was used as primary antibody to notice any physical complex formed between $p27^{Kip1}$ and cyclin E. To determine the functional association of pRb1/107 and pRb2/130 with E2F, anti-p107 and anti-p130 monoclonal antibody were used to immunoprecipitate the complex and the membranes were probed with anti-E2F antibody (Santa Cruz).

Luminescent-based kinase assay

The kinase activity of CDK4 was measured using an ATP detection reagent (Kinase-Glo, Promega, Madison, Wisconsin, USA) to quantify residual ATP after the reaction. The luminescent signal is correlated with the amount of ATP present and is inversely correlated with the amount of kinase activity. Immnuoprecipitated CDK4 was used to perform the kinase assay. The immunoprecipitates were washed three times in a lysis buffer and three times in a kinase buffer (20 mmol/l Tris pH 7.5, 4 mmol/l $MgCl_2$). The assay was performed in 96 multiwell plates in 0.5 µmol/l ATP in an assay buffer consisting of 25 mmol/l HEPES (pH 7.5), 10 mmol/l $MgCl_2$, 5 mmol/l $MnCl_2$, 50 mmol/l KCl, 0.2% bovine serum albumin, 100 µmol/l Na_3VO_4, 0.5 mmol/l DTT, and 1% dimethylsulfoxide. Negative controls (blanks) were reaction mixtures containing no kinase. The kinase reaction mixture was incubated for 90 min at room temperature. After incubation, 10 µl of the ATP detection reagent diluted in the reconstitution buffer was added to the assay plates, incubated at room temperature for 15 min, and the relative light unit signal was measured on the luminescent mode.

Statistical analysis

The results of flow cytometry and immunoblotting were analyzed using the *t*-test for paired observations. The computed *t* score was then compared with the critical *t* scores with the same d.f. The difference between the paired observations was considered to be significant if the computed *t* equaled or exceeded the critical *t* for the chosen level of significance ($P < a$). On the contrary, the difference was considered not significant if the computed *t* was lower than the critical *t* for the chosen significance level ($P > a$). All results were evaluated statistically by applying the SPSSPC package (version 9.0, SPSS, Chicago, Illinois, USA).

Results

Flow cytometric analysis of DNA content

Propidium iodide staining followed by flow cytometry was used to examine the effect of T11TS on the cell cycle distribution of glioma cells. In each group at least 10 000 events were counted and gated into M1, M2, M3, and M4 where M1 was set for cells in the pre-G_1 phase (less than 2n), M2 for cells in the G_1 phase (2n), M3 indicates S-phase cells (in between 2n and 4n) and M4 indicates cells in the G_2/M phase (4n and above). In normal glial cells cell cycle distribution was about 61.55 ± 3.95%, 21.51 ± 2.7%, and 8.77 ± 2.39% of cells in G_1, S, and G_2/M phases, respectively (Fig. 1 and supplementary data 1). In the ethylnitroso urea (ENU)-induced glioma, 60.04 ± 2.94% of cells were accumulated in the S phase whereas only 12.84 ± 1.8% of cells were accumulated in the G_1 phase. T11TS caused accumulation of cells in the G_1 phase; the percentage of G_1 cells increased significantly ($P < 0.0001$) from the glioma populations to ET1 (76.15 ± 3.67%). The percentage of cells in the S phase merely showed a concomitant decline and 1.77 ± 0.99% of cells were in the S phase. With the second dose a similar pattern of accumulation was found with 81.75 ± 2.43% cells in the G_1 phase and 2.12 ± 1.68% of cells in the S phase. Finally, in the ET3 a significantly higher ($P < 0.0001$) percentage of cells (24.48 ± 3.79%) was gated within pre-G_1 phase or apoptotic phase compared with all the other groups. Approximately 66.11 ± 4.35% of cells were found in the G_1 phase and 8.05 ± 3.10% cells in the S phase of the cell cycle. The above results indicate that T11TS induces phase arrest of glioma cells at the G_1 phase of the cell cycle.

Fig. 1

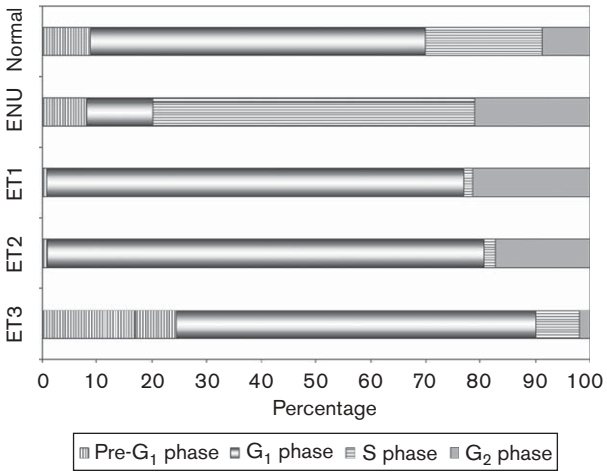

Cell phase distribution study. Cell cycle profiles obtained by propidium iodide staining and subjected to the DNA content analysis using fluorescence-activated cell sorting. Experimental groups were normal, ethyl nitrosourea (ENU), ET1, ET2, and ET3. The percentages of cells in each phase of the cell cycle were calculated using the CellQuestPro software. The graph represents the percentage of cells in each phase of the cell cycle in the 100% stack bar comparing the percentage of each value. Mean values were calculated from the results of three independent experiments (animals: $n = 4$ per group).

Study of the cell cycle proliferation marker

Encouraged by the cell phase distribution study, the PCNA protein level was measured by flow cytometry and immunoblotting. Approximately 60.29 ± 3.63% normal glial cells were found to be PCNA positive in flow cytometric analysis (Fig. 2a and supplementary data 2).

Fig. 2

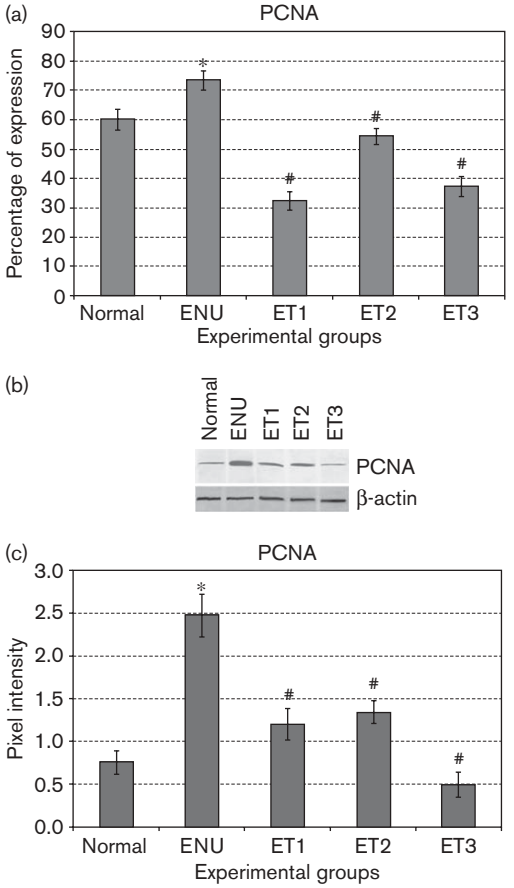

Differential expression of proliferating cell nuclear antigen (PCNA) protein level. (a) Flow cytometric analysis of PCNA percent positive cells. (b) The expression of PCNA protein was analyzed by immunoblotting using anti-PCNA antibody. Actin levels were used to equalize for variation in protein loading in different samples using anti-actin antibody. (c) Pixel intensities of each band were displayed. *Significant increase compared with that of normal control ($P<0.001$). #$P<0.001$ when comparing groups treated with T11TS with ethyl nitrosourea (ENU)-induced glioma group. Column values are mean ± SD from three independent experiments (animals: $n = 4$ per group).

The tumor group showed a high level of PCNA positivity (73.56 ± 3.27%) compared with normal glial cells ($P < 0.0001$) indicating an elevated level of DNA synthesis in altered glial cells. With the first dose of the T11TS the PCNA level decreased significantly ($P < 0.0001$) (32.32 ± 3.27%), indicative of a decrease in DNA synthesis. At the second dose PCNA attained a nearly normal level (54.44 ± 2.71%); however, at the third dose the level of PCNA was decreased considerably (37.3 ± 3.35%) compared ($P < 0.0001$) with glioma. PCNA maintained a below-normal level in T11TS-mediated cell cycle arrest. A similar pattern of results was obtained when PCNA levels were visualized by immunoblotting depicted in Fig. 2b and c. PCNA showed significantly ($P < 0.0001$) higher expression in neoplastic glial cells (2.481 ± 0.025) compared to normal glial cells (0.76 ± 0.14). The PCNA level showed a sharp reduction (1.205 ± 0.19) in ET1 but did not show any alteration ($P > 0.05$) in ET2 (1.345 ± 0.14). After ET3 or the third dose the PCNA level (0.496 ± 0.15) decreased even below normal level (0.76 ± 0.14).

The effect T11TS over the expression of early G_1-phase positive regulators

Cell cycle progression is controlled by cyclins and CKIs, which determine the activity of CDKs [13]. The levels of cyclins are controlled both by transcriptional and post-transcriptional mechanisms; therefore, the protein levels of G_0/G_1 cyclins D1, D2, and D3 and respective CDKs were analyzed by flow cytometry and immunoblotting. Flow cytometry (Fig. 3a and supplementary data 3) illustrated that the cyclin D1 level was increased significantly ($P < 0.01$) in the neoplastic ENU-induced glioma cells (16.36 ± 1.35%) than in the normal glial cells (12.26 ± 1.23%), although in the ET1 the cyclin D1 level was inclined to be lower (13.97 ± 1.2%) but in ET2 the level (5.54 ± 1.28%) showed a sharp downfall ($P < 0.0001$) compared with glioma. After the third dose, cyclin D1 (13.52 ± 1.52%) reached normal levels ($P > 0.05$). Unlike D1, cyclin D2 did not show any increase in the ENU-induced glioma state (11.26 ± 1.45%) compared with normal glial cells (11.21 ± 1.39%). With the administration of the dose of T11TS the cyclin D2 level (10.13 ± 2.27%) did not deviate from glioma. In ET2 (11.23 ± 1.68%) and ET3 (10.57 ± 1.51%) the cyclin D2 level was significantly unaltered compared with other groups. The cyclin D3 protein level was significantly ($P < 0.0001$) increased in the glioma state (18.49 ± 1.55%) compared with the normal glial cells (10.58 ± 1.4%), which showed a sharp decrease in ET2 (5.35 ± 1.26%). The CDK4 protein level was significantly ($P < 0.01$) increased in glioma (17.29 ± 1.22%) when judged against the normal glial cell (11.34 ± 1.49%). Similarly, the CDK6 protein level was also significantly ($P < 0.001$) amplified in glioma (15.65 ± 1.42%) in contrast to the normal glial cells (9.96 ± 1.8%), but the CDK4 and CDK6 levels were not appreciably affected by T11TS treatment ($P > 0.05$) when compared with glioma cells isolated from tumor groups.

Immunoblot analysis (Fig. 3b and c) confirmed a sharp decrease in the cyclin D1 protein level (1.103 ± 0.11) occurring after the first dose of T11TS in comparison with the normal glial cells (0.694 ± 0.1). Cyclin D1 was reduced further after ET2 (0.595 ± 0.09) and attained a normal level that remained unchanged following the third dose (0.857 ± 0.08). Cyclin D2 expression was not significantly increased ($P > 0.05$) in the glioma state (0.802 ± 0.13) compared with the normal glial cells (0.815 ± 0.09), which remained unaltered ($P > 0.05$) after the administration of T11TS. Cyclin D3 showed a similar pattern of results as depicted by cyclin D1. The cyclin D3 protein level was significantly

Fig. 3

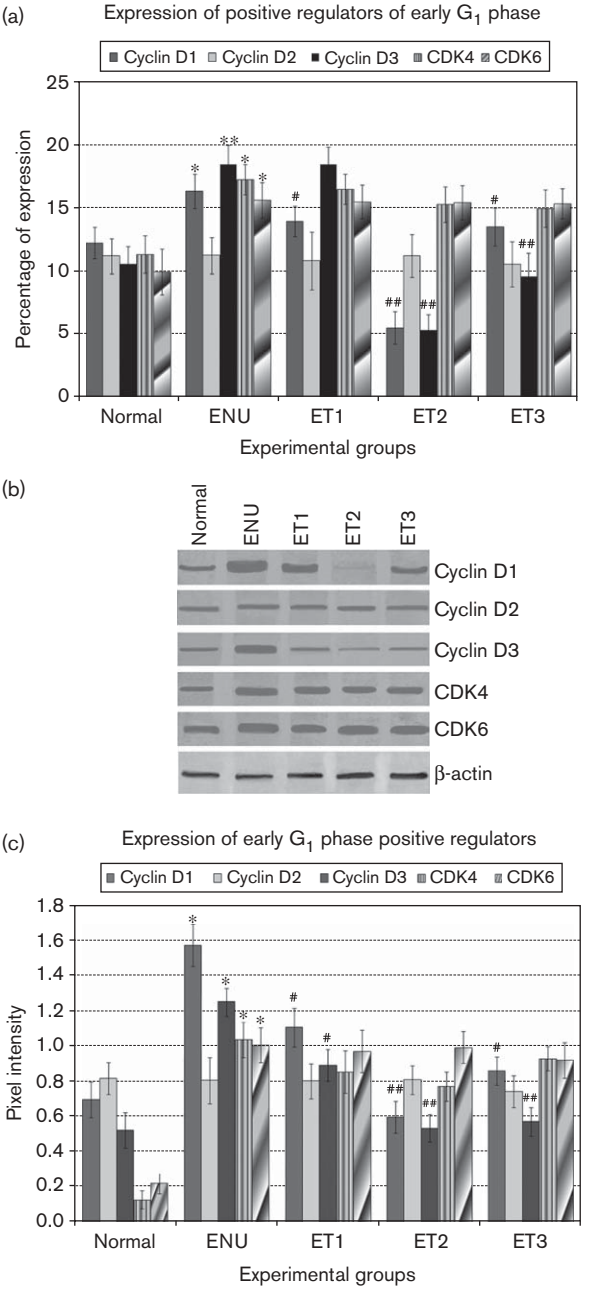

Effect of T11TS on early G_1 cell cycle positive regulators in glioma cells. (a) Flow cytometric analysis of cyclin D1, cyclin D2, cyclin D3, CDK4, and CDK6 percent positive cells. (b) The expression of cyclin D1, cyclin D2, cyclin D3, CDK4, and CDK6 protein levels were analyzed by immunoblotting. Actin levels were used as loading control using anti-actin antibody. (c) Pixel intensities of each band were displayed. *Significant increase compared with that of normal control ($P<0.01$). $^{\#}P<0.05$, $^{\#\#}P<0.001$ when comparing groups treated with T11TS with ethyl nitrosourea (ENU)-induced glioma group. Column values are mean ± SD from three independent experiments (animals: $n = 4$ per group).

decreased in ET1 (0.889 ± 0.09) and attained an almost normal level (0.520 ± 0.1) after ET2 (0.532 ± 0.78). Protein levels of CDK4 and CDK6 were significantly upregulated ($P < 0.0001$) during uncontrolled division in the glioma state (1.034 ± 0.1 and 1.003 ± 0.01) compared with the normal glial cells. But no further significant changes were observed in CDK4 and CDK6 protein levels after the administration of the T11TS.

Expression patterns of the late G_1-phase positive regulators after T11TS treatment

Cyclin E with its catalytic partner CDK2 enters into the cell cycle at a late G_1 phase. The activity of the cyclin E–CDK2 complex peaks at the G_1–S transition [35]. Flow cytometric data (Fig. 4a and supplementary data 4) indicate that the cyclin E protein level was significantly ($P < 0.0001$) upregulated in glioma (38.52 ± 2.82%) compared with the normal glial cells (10.94 ± 3.05%). With the administration of T11TS the cyclin E level decreased consecutively in all the subsequent doses. A significant ($P < 0.05$) decrease was observed in ET1 (35.30 ± 2.94%). A successive decrease in the cyclin E level was noted in ET2 and ET3 (27.47 ± 2.19% and 21.23 ± 1.8%, respectively), but was not able to attain the normal level. The CDK2 level was significantly elevated ($P < 0.0001$) in the glioma cells (17.56 ± 2.03%) but did not attain any significant ($P > 0.05$) changes after T11TS induction.

Immunoblot data (Fig. 4b and c) showed a similar sort of expression pattern as in the flow cytometric studies. ENU-induced glioma cells showed a sharp increase in the cyclin E protein level (4.143 ± 0.27) compared with the normal glial cells (1.703 ± 0.28). T11TS administration induced gradual reduction in the cyclin E protein level, it being the lowest in ET3 (2.365 ± 0.026), but unable to attain normal level. CDK2 was significantly ($P < 0.0001$) upregulated in glioma (0.615 ± 0.15) compared with normal glial cells (0.256 ± 0.07), but T11TS administration did not exert any effect over CDK2 expression as the protein level remained unaltered in all three consecutive doses of T11TS.

The effects of T11TS over the expression of the G_1-phase negative regulators

$p16^{INK4a}$, the founding member of INK4 family protein can antagonize the assembly of cyclin D-dependent kinase by binding to CDK4 and CDK6 [35]. Flow cytometric analysis (Fig. 5a and supplementary data 5) showed the p16 protein level to be significantly ($P < 0.0001$) lowered in glioma (3.63 ± 1.48%) compared with the normal glial cells (16.35 ± 1.46%), but even after the administration of T11TS, the protein level was not able to reach a normal value. Immunoblot data in Fig. 5b and c depicted a similar pattern of results as the p16 band was completely absent in glioma, which faintly reappeared in ET1 (0.577 ± 0.03), but was not detectable in ET2 and again reappeared in ET3 but the level was not able to reach normality. The $p21^{Cip1}$ level was monitored in glial cells isolated from different groups.

Fig. 4

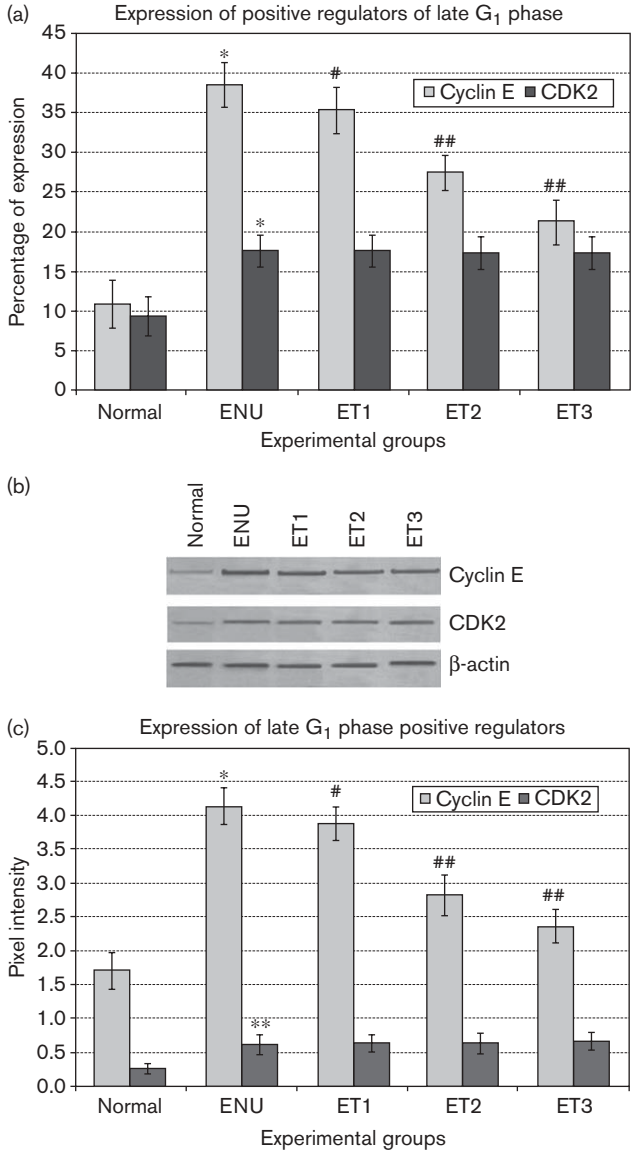

Effect of T11TS on late G_1 cell cycle positive regulators in glioma cells. (a) Flow cytometric analysis of cyclin E and CDK2 percent positive cells. (b) The expression of cyclin E and CDK2 protein levels were assayed by immunoblotting. Actin levels were used to equalize for variation in protein loading in different samples using anti-actin antibody. (c) Pixel intensities of each band were displayed. *Significant increase compared with that of normal control ($P<0.0001$). $^{\#}P<0.05$, $^{\#\#}P<0.001$ when comparing groups treated with T11TS with ethyl nitrosourea (ENU)-induced glioma group. Column values are mean ± SD from three independent experiments (animals: $n = 4$ per group).

Fig. 5

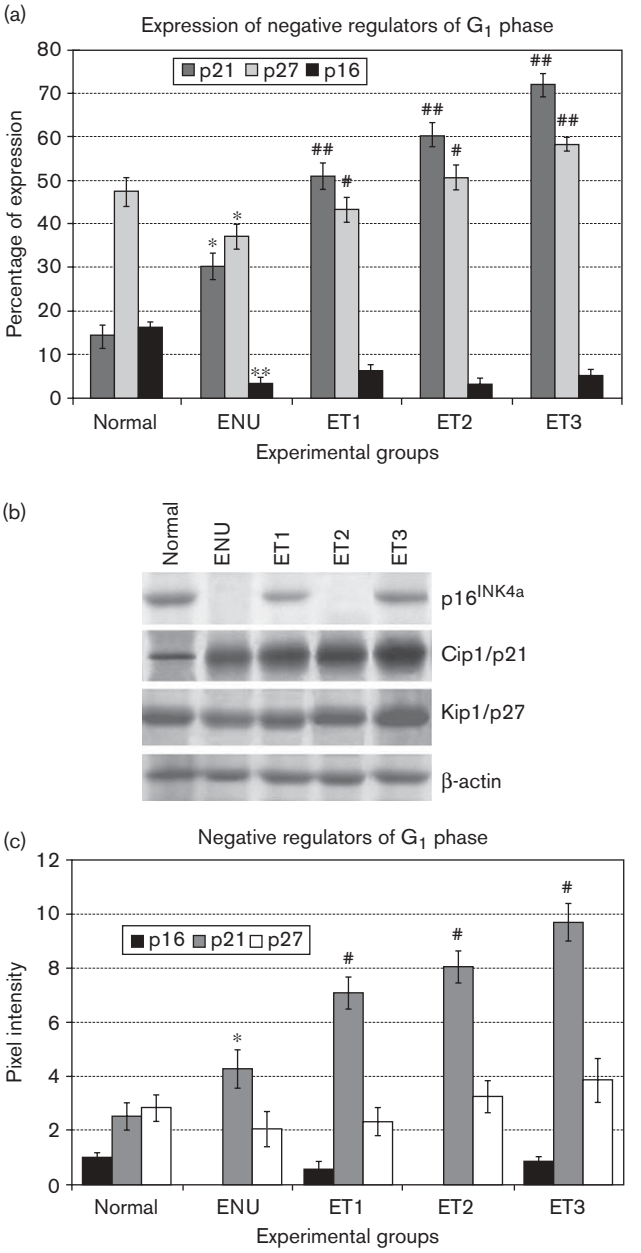

Effect of T11TS on G_1-phase negative regulators in glioma cells. (a) Flow cytometric analysis of p16, $p21^{Cip1}$, and $p27^{Kip1}$ percent positive cells. (b) The expression of p16, $p21^{Cip1}$, and $p27^{Kip1}$ proteins were assayed by immunoblotting. Actin levels were used to equalize for variation in protein loading in different samples using anti-actin antibody. (c) Pixel intensities of each band were displayed. *($P<0.01$) and **($P<0.0001$) denote significant increase compared with that of normal control. $^{\#}P<0.01$, $^{\#\#}P<0.001$ when comparing groups treated with T11TS with ethyl nitrosourea (ENU)-induced glioma group. Column values were mean ± SD from three independent experiments (animals: $n = 4$ per group).

From flow cytometric analysis (Fig. 5a and supplementary data 5) it was found that in the glioma the $p21^{Cip1}$ level (30.54 ± 3.02%) was increased significantly ($P < 0.0001$) compared to normal glial cells (14.49 ± 2.71%). The $p21^{Cip1}$ level was increased sharply in ET1 (51.14 ± 3.01%) compared with the glioma. The $p21^{Cip1}$ level was further increased in ET2; however, it increased immensely showing a heightened ($P < 0.0001$) response after the administration of the third dose (71.94 ± 2.65%).

From the immunoblot data (Fig. 5b and c) it was also evident that the $p21^{Cip1}$ protein level was raised in glioma (2.539 ± 0.71) as the band became intensified ($P < 0.001$) compared with the normal glial cells (2.539 ± 052). The $p21^{Cip1}$ level was increased significantly in all consecutive doses of T11TS with greater enhancement being observed in ET3 (9.74 ± 0.72).

Fig. 6

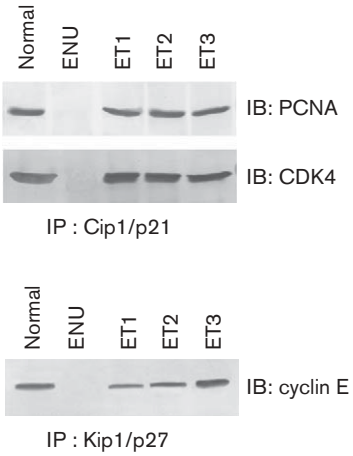

T11TS induces physical association of $p21^{Cip1}$–CDK4, cyclin E-$p27^{Kip1}$, and $p21^{Cip1}$–proliferating cell nuclear antigen (PCNA): showing noticeable $p21^{Cip1}$–PCNA, $p21^{Cip1}$–CDK4, and cyclin E–$p27^{Kip1}$ association in T11TS groups. Cell lysates were immunoprecipitated with anti-p21 and anti-p27 antibodies and immunoblotted with corresponding antibody shown in the panel. Representative of three independent experiments are shown. ENU, ethyl nitrosourea.

The $p27^{Kip1}$ level was significantly ($P < 0.0001$) lowered in the ENU-induced glioma (37.28 ± 2.76%) compared with normal glial cells (47.49 ± 3.26). Gradual upregulation of the $p27^{Kip1}$ protein level was observed both in flow cytometric and immunoblot assays, which reached the peak at ET3 but the fold increase was less than for $p21^{Cip1}$. The $p27^{Kip1}$ level showed the highest response in ET3 (58.34 ± 1.61). Immunoblot analysis also showed that the $p27^{Kip1}$ level increased gradually after T11TS induction – as in the ET1 level it increased to 2.341 ± 0.61 – and in the ET3 level a significant elevation was observed (3.876 ± 0.8).

Physical association of Cip1/p21 with CDK4 and proliferating cell nuclear antigen and Kip1/p27 with cyclin E

CDK4-$p21^{Cip1}$ association was completely absent in glioma cells but reappeared in ET1 and the association was much more intense compared with normal association as evident from the study (Fig. 6). The PCNA–$p21^{Cip1}$ physical association became more conspicuous in the T11TS-administrated groups, whereas this association was not

Fig. 7

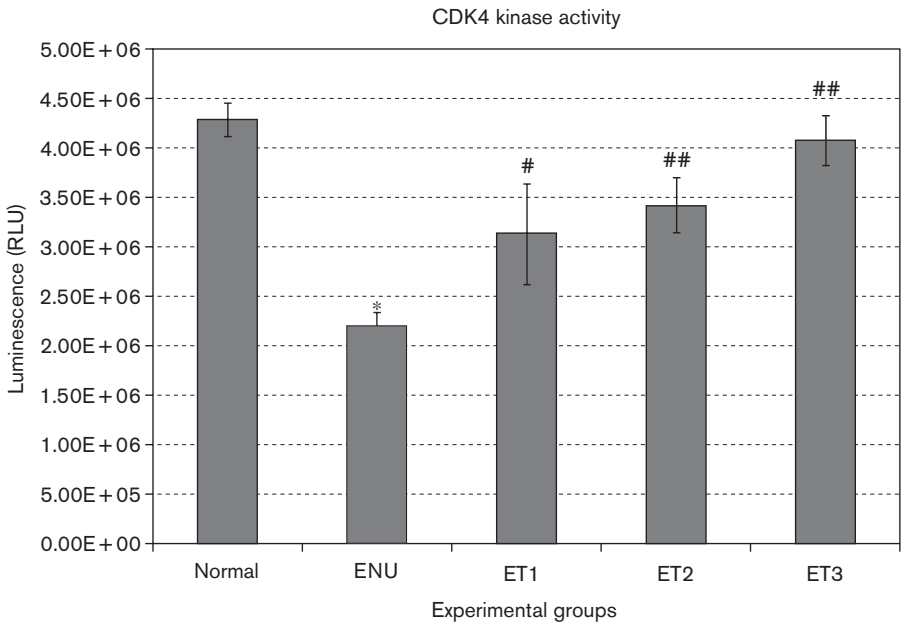

Luminescent-based CDK4 assay. CDK4 activity was measured using an ATP detection reagent to quantify residual ATP after the reaction. The luminescent signal is correlated with the amount of ATP present and is inversely correlated with the amount of kinase activity. CDK4 immnuoprecipitated as described above was used to perform the kinase assay. Relative light unit (RLU) signal was measured on the luminescent mode. *Significant increase compared with that of normal control ($P < 0.0001$). $^{\#}P < 0.001$, $^{\#\#}P < 0.0001$ when comparing groups treated with T11TS with ethyl nitrosourea (ENU)-induced glioma group. Column mean of 10 replicate wells from three independent experiments (mean ± SD; animals: $n = 4$).

visible in glioma cells. After T11TS treatment $p27^{Kip1}$–cyclin E association increased strongly (Fig. 6) correlating with increased expression of these CDKIs.

Fig. 8

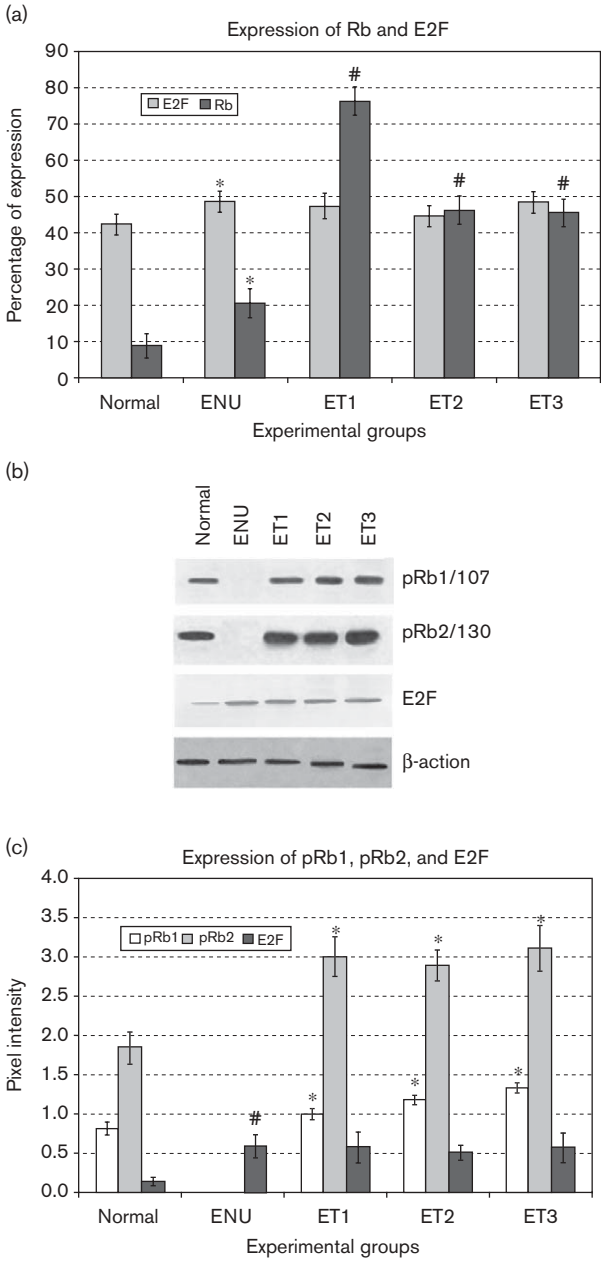

Effect of T11TS on protein level of total retinoblastoma (Rb), hypophosphorylated-Rb, and E2F in glioma cells. (a) Flow cytometric analysis of total Rb and E2F percent positive cells. (b) The expression of hypophosphorylated pRb1/p107, pRb2/p130, and E2F proteins were assayed by immunoblotting. Anti-p107 and anti-p130 used were specific for the detection of hypophosphorylated form of Rb proteins. Actin levels were used as loading control using anti-actin antibody. (c) Pixel intensities of each band were displayed. *Significant increase compared with that of normal control ($P<0.01$). $^{\#}P<0.05$, $^{\#\#}P<0.001$ when comparing groups treated with T11TS with ethyl nitrosourea (ENU)-induced glioma group. Column values are mean ± SD from three independent experiments (animals: $n = 4$).

Decrease in CDK4 activity

CDK activity is one of the determinants of cell cycle progression. As we found increased functional association between $p21^{Cip1}$ and CDK4, the next question to be answered is whether this association has any functional effect over the kinase activity of CDK4. CDK4 from glioma cells showed a low level of ATP remaining after the reaction compared with normal glial cells (Fig. 7). As described above the luminescent signal is correlated with the amount of ATP present and is inversely correlated with the amount of kinase activity. The residual ATP level increased after T11TS administration indicating lowered kinase activity of CDK4, which reached the lowest level with the third dose of T11TS. These results suggest that $p21^{Cip1}$ might effectively block CDK4 activity after T11TS administration.

T11TS increases levels of pRb1/p107 and pRb2/p130, and their binding with E2F

As T11TS showed a strong decrease in the cyclin D (1 and 3) level as well as increased binding of $p21^{Cip1}$, $p27^{Kip1}$ with CDK4 and cyclin E, respectively, our next focus was to investigate the expression of total Rb and hypophosphorylated form of Rb family proteins pRb1/p107 and pRb2/p130. T11TS treatment of glioma cells in three consecutive doses showed an increase in total pRb (Fig. 8a and supplementary data 6) and hypophosphorylated pRb1/p107 and pRb2/p130 protein levels (Fig. 8b and c). Next, E2F protein levels was examined, as E2Fs are the target transcription factors in this pathway which regulate the transcription of growth responsive genes. T11TS treatment did not show any observable change in the E2F protein level. Protein

Fig. 9

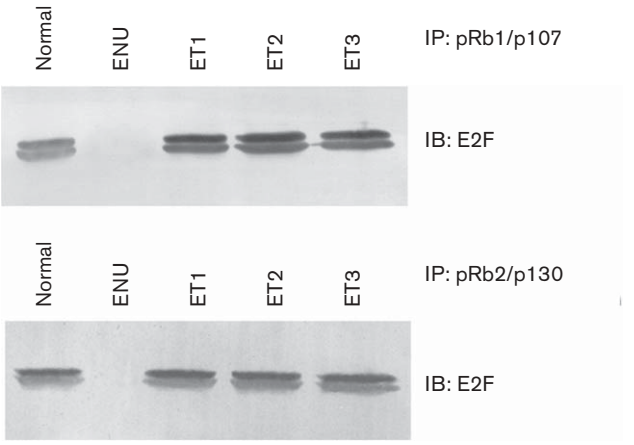

T11TS induces physical association of retinoblastoma protein (pRb1)/p107–E2F and pRb2/p130–E2F showing conspicuous binding of pRb/p107 and pRb2/p130 with E2F in T11TS administered groups. Cell lysates were immunoprecipitated with anti-p107 and anti-p130 antibodies and immunoblotted with anti-E2F antibody shown in the panel. Representative experiments from three independent experiments are shown.

loading was checked by reprobing the same membrane with an actin antibody (Fig. 8b). The oncogenic activity of E2Fs is dependent on their free/bound ratio with pRb-related proteins in pRb lacking cells; therefore, the bound levels of E2F, with pRb1/p107 and pRb2/p130, were determined before and after T11TS treatment. T11TS showed an increased binding of E2F with pRb1/p107 and pRb2/p130, as compared with that of normal glial cells (Fig. 9). The observed effect of T11TS on an induction of this complex level could be of greater significance in defining a mechanistic rationale involved in T11TS-caused G_1 arrest and cell growth inhibition.

Discussion

The major finding of this study is that T11TS strongly induces $p21^{Cip1}$ and $p27^{Kip1}$ and inhibits cyclin D (1 and 3) followed by an increase in hypophosphorylated levels of pRb1/p107 and pRb2/p130, and their increased binding with E2F. These molecular effects of T11TS could be one of the possible underlying mechanisms that resulted in the inhibition of cell growth and G_1 arrest in glioma cell cycle progression.

Our earlier studies showed that T11TS administration caused the activation of the immunocytes with the modulation of the Th1 and Th2 cytokine balance and release of TNF-α, causing apoptosis of glioma cells by an extrinsic pathway in later stages of treatment [32].

An understanding of the organization of cell cycle events is of utmost importance to device-effective therapeutic strategies for cancer [36,37].

The results obtained from the cell phase distribution study (Fig. 1) provide convincing evidence that T11TS exerts its effects on cell cycle progression of glioma cells by accumulating at G_1 phase in ET1 and ET2. When cell cycle phase distributions are compared with alterations in cell cycle regulatory molecules, a strong increase in CDKIs ($p21^{Cip1}$ and $p27^{Kip1}$) (Fig. 5) can be attributed as one of the major causes of T11TS-induced G_1 arrest and cell growth inhibition along with the sharp decrease in the cyclin D (1 and 3) level (Fig. 3). As the expression of D-type cyclins depends upon cell lineages [7,13], cyclin D2 is weakly expressed and shows no marked relationship with any aspect of gliomagenesis [38]. Lower expression of cyclin D2 was found in a small fraction of the gliomas, but its labeling indices did not vary significantly with grade [38]. Consistent with this reports cyclin D2 expression was not significantly increased in ENU-induced glioma cells as evident from the flow cytometry and immunoblotting studies (Fig. 3). Cyclin-D1 serves as a regulatory switch in early cell cycle progression [39]. Given the central role of cyclin D1 in the cell cycle, its expression is regulated at several levels including transcriptional induction [40]. A key mediator of proliferation is the Ras/Raf/MEK/ERK/RSK-MSK cascade, and accordingly, sustained activation of this pathway generated ectopically has been linked to cyclin D1 induction and cell cycle progression [41,42]. Vascular endothelial growth factor and epidermal growth factor, which stimulate Ras–Raf signaling cascades are also downregulated after T11TS treatment (supplementary data 7), which, in turn, lead to downregulation of cyclin D1 (Fig. 3). The G_1 CDKs play an important role in the integration of the proliferation control signals with the cell cycle machinery. The major G_1-phase CDKs are CDK2, CDK4, and CDK6 and their activity is positively regulated by the cyclins [43,44]. As T11TS treatment does not exert any effect over the expression of CDKs, decrease in cyclin D (1 and 3) level (Fig. 3) constrains the formation of active cyclin D–CDK complex in glioma cells.

The important CDKIs include $p21^{Cip1}$, a universal inhibitor of CDKs whose expression is mainly regulated by the p53 tumor suppressor protein [14], and $p27^{Kip1}$, which is also upregulated in response to antiproliferative signals [45,46]. The increased expression of CDKIs by T11TS is both encouraging and important in the sense that the development of glioma has been associated with decrease in p16 and $p27^{Kip1}$ expression as is evident from this study. The $p21^{Cip1}$ protein level increased significantly ($P < 0.0001$) in glioma compared with the normal glial cells (Fig. 5). The activation of $p21^{Cip1}$, however, depends on Akt-mediated phosphorylation. In another study, the association of $p21^{Cip1}$ with Akt was evident and the level of the phosphorylated form of $p21^{Cip1}$ was higher in the ENU group (supplementary data 8). Nevertheless, the $p21^{Cip1}$ level augmented massively showing heightened response after the administration of T11TS and with successive doses it increased exponentially (Fig. 5). T11TS-induced CDKI upregulation may involve a p53-independent pathway, as mutational inactivation in the *p53* tumor suppressor gene has been observed in ENU-induced central nervous system tumors [47,48]. TNF-α induces cell arrest by increasing transcriptional upregulation and stabilization of the $p21^{Waf1}$ protein in the p53-mutated cell through the p53-independent pathway [49]. Our earlier studies showed high TNF-α production after T11TS administration in glioma-bearing rats [50], which can be directly correlated with a sharp rise in the $p21^{Cip1}$ level after T11TS application in ENU-induced glioma cells having mutated *p53*.

Simultaneously, CDK4 activity was measured by the luminescent method (Fig. 7). From the study it is evident that CDK4 activity was highest in the ENU-induced glioma state, which actively phosphorylates the pRb. T11TS do not exert any effect over the expression of the CDK4 protein (Fig. 3) but CDK4 activity was gradually lowered reaching normal level in the third dose of T11TS. In coimmunoprecipitation studies in which CDK4s were immunoprecipitated using $p21^{Cip1}$, total

disappearance of CDK4 in the glioma state was found indicating no functional association with $p21^{Cip1}$ (Fig. 6). Fascinatingly, the association becomes more intense after the administration of T11TS, which was clearly visible as immunoprecipitated CDK4 bands became intensified, providing the molecular mechanism behind the lowering of the CDK4 activity.

By forming a specific binary complex with CDK4, $p21^{Cip1}$ prevents the association of this CDK with cyclin D and thus results in the inhibition of pRb-dependent cell cycle progression in G_1. $p21^{Cip1}$ is unique among the known CKIs in that it not only interacts with the cyclin–CDK complexes, but also interacts and inhibits DNA polymerase auxiliary factor PCNA, which is essential for DNA replication [23,24,51]. Our observations also suggest that because upregulated $p21^{Cip1}$ is associated with PCNA, it inhibits PCNA-dependent DNA replication (Fig. 6). The T11TS-induced upregulated $p27^{Kip1}$ protein may also play a part in this delayed G_1–S transition as the CDKI regulates the G_1–S-phase transition by inhibiting the CDK2/cyclin E complex (Fig. 6).

The pRb-related proteins, pRb1/p107 and pRb2/p130, bind to and modulate the activity of the E2F family of transcription factors hence regulating cell cycle progression through the S phase [52,53]. Consistent with these reports, T11TS caused a decrease in CDK–cyclin complex formation and increased the hypophosphorylated levels of Rb-related proteins and their increased binding with E2Fs (Figs 8 and 9). This may be attributed to lowered expression of growth responsive genes and subsequent growth inhibition of glioma cells by T11TS.

Conclusion

The positive outcome of such an in-vivo study might form a strong basis for the development of T11TS as an anticancer agent. The main new finding in this paper is that the initiation of T11TS-induced cell cycle arrest in glioma cells is preceded by the downregulation of cyclin D1 levels and upregulation of $p21^{Cip1}$. Although this study has drawn a schematic blueprint of T11TS-associated regulation of cell cycle control proteins in glioma cells, the molecular mechanism for the T11TS-induced regulation of cyclins, CDKs, and CKIs warrants further investigation.

Acknowledgements

S Acharya is grateful to the Council of Scientific and Industrial Research (CSIR), Govt. of India for providing the research fellowship [F. No. 9/951/ (02) EMR-I 2005]. The authors thank Dr Mitali Chatterjee of Dept. of Pharmacology, IPGME and R, Kolkata, for providing us with the flow cytometry facility. The authors also thank Prof Debjani Chakraborty of Department of Physiology, IPGME and R, Kolkata, for encouragement and helpful cooperation. Grant support: Council for Scientific and Industrial Research (CSIR), Govt. of India.

References

1 Maher EA, Furnari FB, Bachoo RM, Rowitch DH, Louis DN, Cavenee WK, *et al.* Malignant glioma: genetics and biology of a grave matter. *Genes and Dev* 2001; **15**:1311–1333.
2 Morgan DO. Cyclin-dependent kinases: engines, clocks, and microprocessors. *Annu Rev Cell Dev Biol* 1997; **13**:261–291.
3 Kopnin BP. Targets of oncogenes and tumor suppressors: key for understanding basic mechanisms of carcinogenesis. *Biochemistry* 2000; **65**:2–27.
4 Lukas J, Bartkova J, Rohde M, Strauss M, Bartek J. Cyclin D1 is dispensable for G_1 control in retinoblastoma gene-deficient cells independently of CDK4 activity. *Mol Cell Biol* 1995; **15**:2600–2611.
5 Lukas J, Parry D, Aagaard L, Mann DJ, Bartkova J, Strauss M, *et al.* Retinoblastoma-protein-dependent cell-cycle inhibition by the tumor suppressor p16. *Nature* 1995; **375**:503–506.
6 Ohtsubo M, Theodoras AM, Schumacher J, Roberts JM, Pagano M. Human cyclin E, a nuclear protein essential for the G_1-to-S phase transition. *Mol Cell Biol* 1995; **15**:2612–2624.
7 Sherr CJ. G_1 phase progression: cycling on cue. *Cell* 1994; **79**:551–555.
8 Ewen ME, Sluss HK, Sherr CJ, Matsushime H, Kato J, Livingston DM. Functional interactions of the retinoblastoma protein with mammalian D-type cyclins. *Cell* 1993; **73**:487–497.
9 Hannon GJ, Demetnck D, Beach D. Isolation of the Rb-related p130 through its interaction with CDK2 and cyclins. *Genes Dev* 1993; **7**:2378–2391.
10 Lundberg AS, Weinberg RA. Functional inactivation of retinoblastoma protein requires sequential modification by at least two distinct cyclin-CDK complexes. *Mol Cell Biol* 1998; **18**:753–761.
11 Harbour JW, Luo RX, Dei Santi A, Postigo AA, Dean DC. CDK phosphorylation triggers sequential intramolecular interactions that progressively block Rb functions as cells move through G_1. *Cell* 1999; **98**:859–869.
12 Hengst L, Gopfert U, Lashuel HA, Reed SI. Complete inhibition of CDK/cyclin by one molecule of $p21^{Cip1}$. *Genes and Dev* 1998; **12**:3882–3888.
13 Sherr CJ, Roberts JM. Inhibitors of mammalian G_1 cyclin-dependent kinases. *Genes and Dev* 1995; **9**:1149–1163.
14 El-Deiry WS, Tokino T, Velculescu VE, Levy DB, Parsons R, Trent JM, *et al.* WAF1 a potential mediator of p53 tumor suppression. *Cell* 1993; **75**:817–825.
15 Dulic V, Kaufmann WK, Wilson SJ, Tlsty TD, Lees E, Harper JW, *et al.* p53-dependent inhibition of cyclin-dependent kinase activities in human fibroblasts during radiation-induced G_1 arrest. *Cell* 1994; **76**:1013–1023.
16 Noda A, Ning Y, Venable SF, Pereira-Smith OM, Smith JR. Cloning of senescent cell-derived inhibitors of DNA synthesis using an expression screen. *Exp Cell Res* 1994; **211**:90–98.
17 Halevy O, Novitch BG, Spicer DB, Skapek SX, Rhee J, Hannon GJ, *et al.* Correlation of terminal cell cycle arrest of skeletal muscle with induction of p21 by MyoD. *Science* 1995; **267**:1018–1021.
18 Macleod KF, Sherry N, Hannon G, Beach D, Tokino T, Kinzler K, *et al.* p53-dependent and independent expression of p21 during cell growth, differentiation and DNA damage. *Genes Dev* 1995; **9**:935–944.
19 Chen J, Jackson PK, Kirschner MW, Dutta A. Separate domains of p21 involved in the inhibition of CDK kinase and PCNA. *Nature* 1995; **374**:386–388.
20 Nakanishi M, Robetorge RS, Pereira-Smith OM, Smith JR. The carboxy-terminal region of p21SDI1/WAF1/CIP1 is involved in proliferating cell nuclear antigen binding but does not appear to be required for growth inhibition. *J Biol Chem* 1995; **270**:17060–17063.
21 Chen J, Saha P, Kornbluth S, Dynlacht BD, Dutta A. Cyclin-binding motifs are essential for the function of p21CIP1. *Mol Cell Biol* 1996; **16**:4673–4682.
22 Adams PD, Sellers WR, Sharma SK, Wu AD, Nalin CM, Kaelin WG Jr. Identification of a cyclin-CDK2 recognition motif present in substrates and p21-like cyclin-dependent kinase inhibitors. *Mol Cell Biol* 1996; **16**:6623–6633.
23 Morris GF, Mathews MB. Regulation of proliferating cell nuclear antigen during the cell cycle. *J Biol Chem* 1989; **264**:13856–13864.
24 Kelman Z. PCNA: structure, functions and interactions. *Oncogene* 1997; **14**:629–640.

25 Flores-Rozas H, Kelman Z, Dean FB, Pan Z-Q, Harper JW, Elledge SJ, *et al*. CDK-interacting protein 1 directly binds with proliferating cell nuclear antigen and inhibits DNA replication catalyzed by the DNA polymerase d holoenzyme. *PNAS* 1994; **91**:8655–8659.

26 Kitao T, Takeshita M, Hattori K. Studies on glycopeptide released by trypsin from sheep erythrocytes. *J Immunol* 1976; **117**:310–312.

27 Sarkar S, Begum Z, Dutta S, Dutta SK, Chaudhuri S, Chaudhuri S. Sheep form of leucocyte function antigen-3 (T11TS) exerts immunostimulatory and anti-tumor activity against experimental brain tumor: a new approach to biological response modifier therapy. *J Exp Clin Cancer Res* 2002; **21**:95–106.

28 Begum Z, Ghosh A, Sarkar S, Mukherjee J, Mazumdar M, Sarkar P, *et al*. Documentation of immune profile of microglia through cell surface marker study in glioma model primed by a novel cell surface glycopeptide T11TS/SLFA-3. *Glycoconj J* 2004; **20**:515–523.

29 Yamashita K, Parish CR, Warren HS, Harrison LC. A multimeric form of soluble recombinant sheep LFA-3 (CD58) inhibits human T-cell proliferation. *Immunology* 1997; **92**:39–44.

30 Lantos PL. Chemical induction of tumors in nervous system. In: Thomas GT, editors. *Neurooncology*. New York, London: Churchill Livingstone; 1993:85–107.

31 Druckray H, Ivancovic S, Preussman R. Tetragenic and carcinogenic effects in the offspring after single injection of ethylnitroso urea to pregnant rats. *Nature* 1966; **210**:1378.

32 Bhattacharjee M, Acharya S, Ghosh A, Sarkar P, Chatterjee S, Kumar P, *et al*. Bax and Bid act in synergy to bring about T11TS-mediated glioma apoptosis via the release of mitochondrial cytochrome c and subsequent caspase activation, Int. *Immunology* 2008; **20**:1489–1505.

33 Colello RJ, Sato-Bigbee C. Purification of oligodendrocytes and their progenitors using immunomagnetic separation and percoll gradient centrifugation. In: Crawley JN, Gerten C, McKay R, Rogawski M, Sibley DR, Skolnick P, eds. *Current protocols in Neuroscience,* Supplement 3. New York: Wiley, 1998: 3.12.1–3.12.14.

34 Weinstein DE. Isolation and purification of primary rodent astrocytes. In: Crawley JN, Gerten C, McKay R, Rogawski M, Sibley DR, Skolnick P, eds. *Current protocols in Neuroscience,* New York: Wiley, 1997: 3.5.1–3.5.9.

35 Sherr CJ. The pezcoller lecture: cancer cell cycle revisited. *Can Res* 2000; **60**:3689–3695.

36 Hunter T, Pine J. Cyclins and cancer II: cyclin D and CDK inhibitors come of age. *Cell* 1994; **79**:573–582.

37 Pardee AB. G_1 events and regulation of cell proliferation. *Science* 1989; **246**:603–608.

38 Zhang X, Zhao M, Huang AY, Fei Z, Zhang W, Wang XL. The effect of cyclin D expression on cell proliferation in human gliomas. *J Clin Neurosci* 2005; **12**:166–168.

39 Stacey DW. Cyclin D1 serves as a cell cycle regulatory switch in actively proliferating cells. *Curr Opin Cell Biol* 2003; **15**:158–163.

40 Hamel PA, Hanley-Hyde J. G_1 cyclins and control of the cell division cycle in normal and transformed cells. *Cancer Insvest* 1997; **15**:143–152.

41 Balmanno K, Cook S. Sustained MAP kinase activation is required for the expression of cyclin D1, $p21^{Cip1}$ and a subset of AP-1 proteins in CCL39 cells. *Oncogene* 1999; **18**:3085–3097.

42 Lavoie J, L'Allemain G, Brunet A, Muller R, Pouyssegur J. Cyclin D1 expression is regulated positively by the p42/p44 MAPK and negatively by the p38/HOGMAPK pathway. *J Biol Chem* 1996; **271**:20608–20616.

43 Harper JW, Elledge SJ, Keyomarsi K, Dynlacht B, Tsai LH, Zhang P, *et al*. Inhibition of cyclin-dependent kinases by p21. *Mol Biol Cell* 1995; **6**:387–400.

44 Toyoshima H, Hunter T. P27 a novel inhibitor of G_1 cyclin-CDK protein kinase activity, is related to p21. *Cell* 1994; **78**:67–74.

45 Tsai LH, Lees E, Faha B, Harlow E, Riabowol K. The CDK2 kinase is required for the G_1 to S transition in mammalian cells. *Oncogene* 1993; **8**:1593–1602.

46 Polyak K, Lee MH, Erdjument-Bromage H, Koff A, Roberts JM, Tempst P, *et al*. Cloning of p27/kip1, cyclin-dependent kinase inhibitor and a potential mediator of extracellular antimitogenic signals. *Cell* 1994; **78**:59–66.

47 Calvert R, Hongyo T, Buzard G. Mutation in p53 gene of transplacentally induced rat gliomas. *Proc Am Assoc Cancer Res* 1994; **35**:1033.

48 Mukherjee J, Ghosh A, Duttagupta AK, Chaudhuri S, Chaudhuri S. Characterization of genomic instability along with p53 mutation in ENU induced brain tumor cells: establishment of apoptogenic role of T11TS/S-LFA3 in genetically altered cells. *Can Biol Ther* 2006; **5**:156–164.

49 Kobayashi N, Takada Y, Hachiya M, Ando K, Nakajima N, Akashi M. TNF-α induced $p21^{waf1}$ but not Bax in colon cancer cells WiDr with mutated p53: important role of protein stabilization. *Cytokine* 2000; **12**:1745–1754.

50 Chaudhuri S, Ghosh A. Glioma therapy: a novel insight in the immunotherapeutic regime with T11TS/SLFA-3. *Cent Nerv Syst Agents Med Chem* 2006; **6**:245–270.

51 Maga G, Hubscher U. Proliferating cell nuclear antigen (PCNA): a dancer with many partners. *J Cell Sci* 2003; **116**:3051–3060.

52 Howard CM, Claudio PP, Luca AD, Stiegler P, Jori FP, Safdar NM, *et al*. Inducible pRb2/p130 expression and growth-suppressive mechanisms: evidence of pRb2/p130, p27kip1, and cyclin E negative feedback regulatory loop. *Cancer Res* 2000; **60**:2737–2744.

53 Paggi MG, Baldi A, Bonetto F, Giordano A. Retinoblastoma protein family in cell cycle and cancer: a review. *J Cell Biochem* 1996; **62**:418–430.